Carbon Trends 19 (2025) 100469

Contents lists available at ScienceDirect

Carbon Trends

journal homepage: www.elsevier.com/locate/cartre

Polarized Raman spectroscopy of aligned DNA-wrapped single-wall carbon nanotubes

Seyedeh Maryam Banihashemian [a,*], Mohsen Mesbah [b,**], Hesam Kamyab [c,d,e,*], Mohammad Mahdi Taheri [f], Balamuralikrishnan Balasubramanian [g]

[a] MEMS & NEMS Laboratory, Faculty of New Sciences & Technologies, University of Tehran, PO Box 14395-1561, Tehran, Iran
[b] Metallurgy Department, Faculty of Engineering, University of Mons, 20, Place Du Parc, Mons, Belgium
[c] Department of Biomaterials, Saveetha Dental College and Hospital, Saveetha Institute of Medical and Technical Sciences, Chennai, 600077, India
[d] The KU-KIST Graduate School of Energy and Environment, Korea University, 145 Anam-Ro, Seongbuk-Gu, Seoul, 02841, Republic of Korea
[e] Faculty of Social Sciences, Media and Communication, University of Religions and Denominations, Pardisan, Qom, Iran
[f] Department of Pharmaceutical Biomaterials, Faculty of Pharmacy, Tehran University of Medical Sciences, Tehran, Iran
[g] Department of Food Science and Biotechnology, College of Life Sciences, Sejong University, Seoul 05006, Republic of Korea

ARTICLE INFO

Keywords:
SWCNT
Thymine
Raman spectroscopy
Polarization
Self-aligned array

ABSTRACT

This study introduces a new method to create highly ordered, self-aligned arrays of single-wall carbon nanotubes (SWCNTs) using short DNA composed of 20 thymine bases, known as Poly(dT)20. The SWCNTs were first functionalized through a chemical treatment involving a mixture of sulfuric acid (H_2SO_4) and nitric acid (HNO_3) in a 3:1 ratio, followed by uniform dispersion achieved via a cold ultrasonic technique. Subsequently, the Poly (dT)20 was wrapped around the SWCNTs using a sonothermal process, with variations in time and temperature to enhance alignment. The structural integrity and alignment of the resulting Poly(dT)20 /SWCNT arrays were characterized using scanning electron microscopy (SEM), and profile meter geometry analysis, all of which confirmed the successful alignment of the SWCNTs. Further analysis through ultraviolet-visible spectroscopy (UV–VIS) and Fourier-transform infrared spectroscopy (FTIR) provided evidence of the bonding interactions between the Poly(dT)20 and SWCNTs. Ennhanced Raman spectroscopy of the Poly(dT)20/SWCNT arrays, conducted with polarized light, revealed a significant dependence of the G-band on the polarization angle, yielding a depolarization ratio of 0.211 and linear relationship between I and $\cos^2(\alpha)$. The HRTEM image confirms that the attachment of 20-mer thymine to single-walled carbon nanotubes (SWCNTs) by wrapping around them introduces steric hindrance, which physically separates the nanotubes and prevents aggregation. This finding indicates a well alignment of the Poly(dT)20/SWCNT arrays. The anisotropic characteristics exhibited by the SWCNTs in conjunction with the Poly(dT)20 as a biomaterials suggest promising applications in various fields, including biomedical components, nano-electronic devices, and bio-optics.

1. Introduction

In recent years, unidirectional nanoscale materials have drawn a lot of interest due to their prospective uses in a variety of industries, such as bioelectronics, activiated carbon, gas sensor technology, and nanomedicine [1–7]. When creating nanoelectronic devices, the anisotropic structure of nanomaterials in systems at the nano and mesoscales presents an alluring challenge [8,9]. Carbon nanotubes (CNTs) are particularly captivating due to their individual properties, notably their high length-to-diameter aspect ratio (cylindrical structure). This unique geometry results in variations in properties along the axial direction compared to the radial direction. Well organization and alignment of single-walled carbon nanotube (SWCNT) clusters are crucial for their effective application in practical scenarios. However, the powerful interactions among single-walled carbon nanotubes (SWCNTs) frequently lead to entanglement and disorder. Scientists have investigated various

* Corresponds authors at: The KU-KIST Graduate School of Energy and Environment, Korea University, 145 Anam-Ro, Seongbuk-Gu, Seoul, 02841, Republic of Korea
** Corresponding author at: Metallurgy Department, Faculty of Engineering, University of Mons, 20, Place Du Parc, Mons, Belgium
E-mail addresses: banihashemian@ut.ac.ir (S.M. Banihashemian), mohsen.mesbah@umons.ac.be (M. Mesbah), khesam2@live.utm.my, hesam_kamyab@yahoo.com (H. Kamyab).

https://doi.org/10.1016/j.cartre.2025.100469
Received 28 August 2024; Received in revised form 14 January 2025; Accepted 15 January 2025
Available online 19 January 2025

techniques to overcome this issue, such as using templates, applying external forces, and modifying chemical properties to align SWCNTs. This includes methods that induce a bipolar moment parallel to the SWCNT axis and techniques that enhance sensitivity and selectivity by combining DNA with SWCNTs [10–17].

The combination of carbon nanotubes (CNTs) with DNA molecules shows great promise for creating unidirectional supermolecule hybrids that leverage the unique properties of nanotubes alongside the exceptional recognition capabilities of DNA [18–24]. Single-walled carbon nanotubes (SWCNTs) stand out among various CNT types due to their exceptional properties, including a high length-to-diameter ratio, extensive surface area, and customizable electronic behavior [25–27]. Raman scattering is one of the principal techniques for studying the essential properties of carbon tubes and biomaterial characterization [28,29]. It has been demonstrated as an effective tool for evaluating the alignment of DNA-wrapped single-wall carbon nanotubes (SWCNTs) [30]. This approach aimed to explore the interactions between the DNA and SWCNTs, focusing on the alignment and orientation of the G-band in Raman spectroscopy. Glamazda et al. conducted intriguing research on the Raman absorption properties of DNA-wrapped single-wall carbon nanotubes (SWCNTs), utilizing a natural polymer derived from 300 nucleotides of chicken DNA that was grafted onto SWCNTs and encapsulated in a gelatin film [31].

Wu et al. (2015) demonstrated the capabilities of angle-resolved polarized Raman spectroscopy in identifying the crystalline orientation of black phosphorus, which could be analogous to the study of light polarization in SWCNT arrays . The insights gained from this technique can provide a deeper understanding of how the alignment of SWCNTs influences their optical properties and how these properties can be effectively measured through Raman spectroscopy [32]. Liu et al. (2020) further highlighted the significance of achieving aligned, high-density semiconducting carbon nanotube arrays to advance electronic applications. Their findings underscore that high purity and density of CNT arrays are vital for effective electronic performance, which correlates with the objective of creating ordered arrays of SWCNTs using DNA [33]. Utilizing machine learning techniques, such as deep learning algorithms, to analyze Raman spectral data for identifying and quantifying oligonucleotide interactions with SWCNTs could enhance the specificity and sensitivity of detection methods [34]. Research indicates that surface-enhanced Raman spectroscopy (SERS) can significantly amplify the Raman signals from oligonucleotides, thus facilitating sensitive detection [35,36]. The integration of self-aligned SWCNTs with oligonucleotides could enhance these SERS effects, improving the detection sensitivity of viral pathogens, as evidenced in studies focused on SERS-based biosensors [37]. Saito et al.,. in 2023 introduces a novel Raman analysis technique that enables the determination of (n,m)-resolved functionalization extents in unsorted SWCNT by analyzing the relative intensities of diameter-specific Raman features [38]. Understanding the defect characteristics of SWCNTs is crucial for optimizing their performance in biosensing applications. Zhang et al. (2023) developed methods for quantifying sp3 defect densities in SWCNTs using Raman spectroscopy, which allows for a deeper understanding of how defects might influence the interaction with oligonucleotides [39]. Golubewa et al. (2024) investigated the cellular uptake and fate of SWCNTs capped with DNA or oligonucleotides in glioma cells using Raman spectroscopy. Their findings revealed a two-phase accumulation mechanism for SWCNT-DNA complexes, involving initial vesicular transport followed by lysosomal degradation [40].

Despite significant advancements in the experimental and theoretical alignment and functionalization of single-walled carbon nanotubes (SWCNTs), achieving a scalable, and application-ready structure for fabricating self-aligned SWCNT arrays using simple molecules, while precisely controlling their sequence, remains a challenge. Light polarized by small arrays of single-walled carbon nanotubes (SWCNTs) decorated with small oligomers has the potential to function as a light switch for controlling material interactions.

This study investigates the grafting of synthetic short oligonucleotide DNA, specifically 20-base DNA (poly(dT)20), onto single-wall carbon nanotubes (SWCNTs) to develop a rapid, straightforward, reliable, and scalable method for fabricating self-aligned SWCNT arrays capable of polarizing light. This approach aims to explore their potential as advanced optical materials for applications in photonics and material interaction studies.To explore the potential applications of these arrays in light polaarization and evaluate the alignment and orientation sensitivity of the SWCNTs, polarized Raman spectroscopy is employed. This approach facilitates the self-alignment of the poly(dT)20/ SWCNT structure into parallel arrays capable of selectively polarizing light. The process begins with the functionalization of SWCNTs using physical and chemical methods. High-resolution microscopic techniques, including scanning electron microscopy (SEM) and high-resolution tunneling electron microscopy (HRTEM), ultraviolet-visible (UV–Vis) and Fourier-transform infrared (FTIR) spectroscopy used to validate the successful bonding interactions between the DNA and SWCNTs. The polarization behavior of the poly(dT)20/ SWCNTs was evaluated by analyzing the Raman spectra at different scattering angles. The Raman spectra, enhanced with polarized light, reveal a significant dependence of the G-band on the polarization angle, with well alignment of the poly(dT)20/ SWCNT arrays. The promising polarization behavior of the Poly(dT)20/ SWCNT structure opens up exciting possibilities for exploring new applications in fields like biosensing, and optoelectronics.

2. Materials and methods

All chemicals used in this study were of analytical grade and sourced from Sigma-Aldrich. Glassware was thoroughly cleaned using a solution of nitric acid (HNO_3) and hydrochloric acid (HCl) in a 3:1 vol ratio, followed by ultrasonic cleaning. Following an extensive wash with doubly distilled water, nitrogen gas was used to dry the glassware. Physical vapor deposition was used to create gold nanoparticles with a diameter of <10 nm. Integrated DNA Technologies (IDT) supplied purification services for the synthesis and purification of a 20-base single-strand DNA homopolymer (20-mer oligo, 25 nmole, 3 OD) made completely of thymine utilizing small-scale polyacrylamide gel electrophoresis (PAGE). The Single-Walled Carbon Nanotubes (SWCNTs) with diameters ranging from 2 to 5 nm were supplied by ALPHA Instrument Company. These SWCNTs have a purity greater than 90 wt%. The length of the nanotubes varies between 5 and 30 μm, and they possess a special surface area of 380 m^2/g. Additionally, the ash content is <1.5 wt%, while the electrical conductivity exceeds 100 s/cm. The total weight of the supplied material is 1855.00 g, and the tap density is measured at 0.14 g/cm^3.

2.1. SWCNT preparation

Typically, a 200 mL mixture of sulfuric and nitric acids in a 2/3 vol ratio was mixed with 50 mg of raw SWCNTs (length-to-diameter ratio = 5000/2). After 15 min of sonication in an ultrasonic bath, the mixture was heated to 80 °C for two hours, then to 25 °C for one hour, 60 °C for three hours, and finally, 25 °C for seventy-two hours. Following treatment, the mixture was centrifuged for 30 min at 4000 rpm after being diluted with deionized water (DI, 16 MΩ). Filtering through a pore membrane with a pore size of 0.2 μm came after the treatment. After being cleaned with deionized water, the product was dried for a day at 70 °C in a vacuum furnace (Fig. 1). SWCNTs are forced to have a free-standing form when SWNT bundles are ultrasonically treated in ice and DI water.

2.2. Poly(dT)20 and SWCNT congugation

After vortexing the tubes for 20 s, 25 μL of the poly(dT)20 was diluted with 1.5 mL deionized (DI) water and mixed with the treated SWCNTs and incubated for an hour. For ten minutes, the poly(dT)20 and

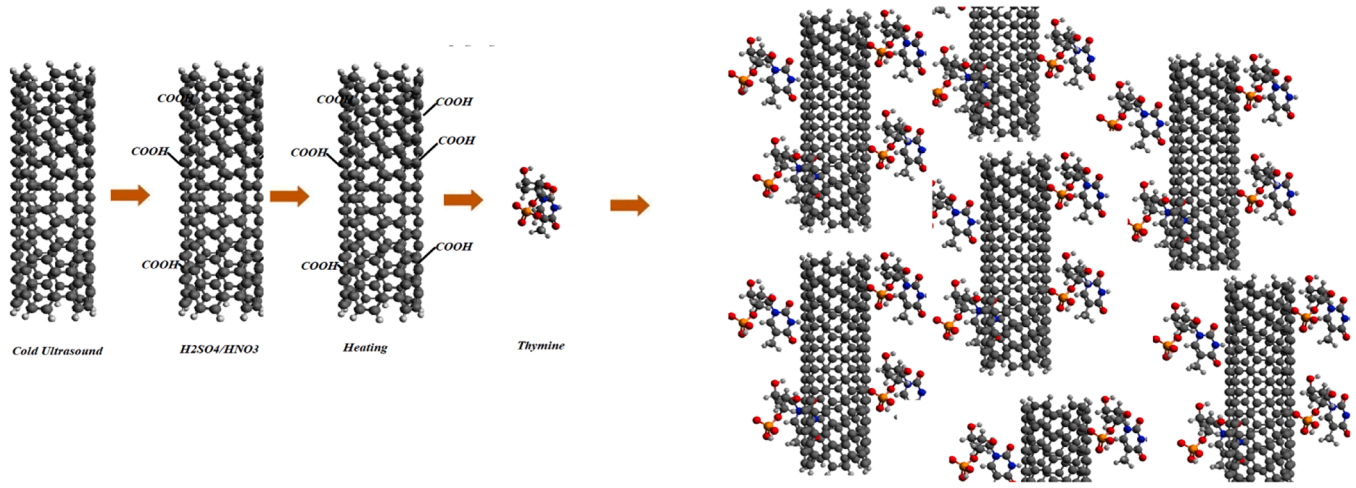

Fig. 1. Schematic of poly(dT)20-wrapped SWCNTs on a glass substrate.

SWCNT combination with a 1:1 concentration ratio was subjected to further ultrasonic treatment in ice. The SWCNT-poly(dT)20 solution was then centrifuged and vorteced alternatively three times. In order to verify that poly(dT)20 had successfully bound to the SWCNTs, the final solution was prepared for characterisation. All measurements were carried out under ambient conditions, with a room temperature of approximately 25 −27 °Celsius and a relative humidity of 53 %.

2.3. Characterization and instruments

The produced poly(dT)20/SWCNT was placed on a 1 cm x 1 cm piece of glass that had been plasma treated, and it was allowed to dry at a steady state temperature while air was flowing. Using a Ranishwa micro Raman 514 nm, Perkin Elmer 750, Hitachi H-7100® electron microscopy (Hitachi High-Technologies Corporation, Tokyo, Japan), and Philips (X'pert, Cu Kα) instruments, respectively, Raman spectroscopy, ultraviolet-visible (UV–Vis) spectroscopy, transmission electron microscopy (TEM), and field emission electron microscopy (FESEM) were used to characterize Poly(dT)20/SWCNT. The setup was prepared and the angle dependency of the spectrum was assessed using a Focal Lenz, Quadra and half wave plates, polarizer, and rotation stage. By examining the Raman spectra at various scattering angles, the sample's polarization behavior was evaluated.

3. Results and discussion

3.1. Raman spectroscopy

The Raman spectra of SWCNTs and poly(dT)20 /SWCNT were evaluated using a polarized confocal Raman microscope with a 514 nm laser. The laser light was focused onto SWCNTs and the parallel-aligned SWCNTs (poly(dT)20 /SWCNT) using a 20x objective. As depicted in the Fig. 2, a small shift in the G band from 1583.97 cm^{-1} to 1591.95 cm^{-1} and in the 2D band from 2679.71 cm^{-1} to 2695,09 cm^{-1} is observed in the Raman peaks of single-walled carbon nanotubes (SWCNTs) when they are attached to the poly(dT)20. This shift can be primarily attributed to several factors, including charge transfer interactions, mechanical strain, alterations in the local environment, anisotropic properties, and the potential formation of new vibrational modes. Together, these factors influence the vibrational characteristics of the SWCNTs, leading to noticeable shifts in the Raman spectrum. The anisotropic changes are particularly significant, as evidenced by the angle-dependent behavior of the Raman signals explored in this study. Furthermore, the alignment of the poly(dT)20/SWCNT complex can greatly impact the polarization of the Raman signal.

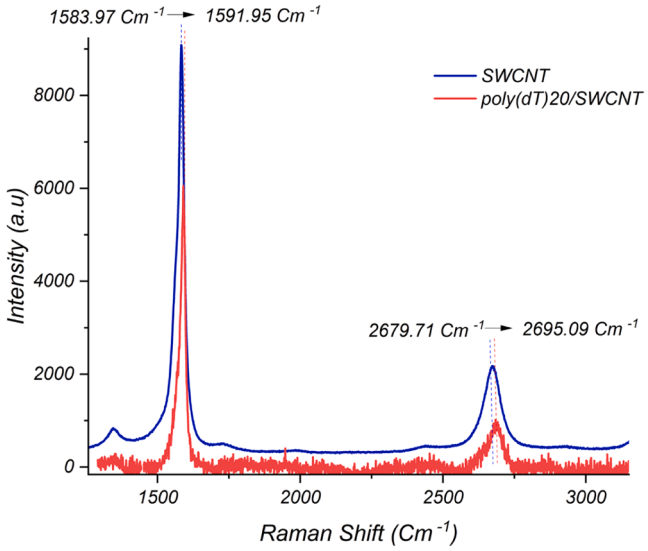

Fig. 2. Raman spectra of SWCNT and poly(dT)20 /SWCNT (The blue arrows indicate the direction of the peak shift).

3.2. Image analysis

3.2.1. Scanning electron microscope (SEM)

A 3D pattern of poly(dT)20/SWCNT samples was captured using a profilometer (Fig. 3(a)), revealing a parallel pattern with a periodicity of 10 μm and a closely uniform array. Additionally, the SEM image in Fig. 3 (b) demonstrates that poly(dT)20 and SWCNT have established a parallel alignment of the carbon nanotube arrays.

3.2.2. HRTEM image

Fig. 4(a) displays the HRTEM image of the Poly(dT)20/SWCNT structure, revealing the wrapping of short-length Poly(dT)20 around the SWCNTs. Fig. 4(b) offers a magnified view of Fig. 4(a) to facilitate a more detailed analysis. The yellow parallel lines in the Fig. 4(b) are drawn in the direction of the array alignment, illustrating a parallel arrangement of the SWCNTs (Fig. 4(b)).The HRTEM image also confirms the localization of short length poly(dT)20 wrapped on the SWCNT walls that can plays as a spacer role to prevent agglomeration of AWCNTs and form an well alignment (red arrow in the Fig. 4(b)). The attachment of 20-mer thymine to SWCNTs, offers a strategy to mitigate nanotube aggregation which creates a steric hindrance effect physically separating

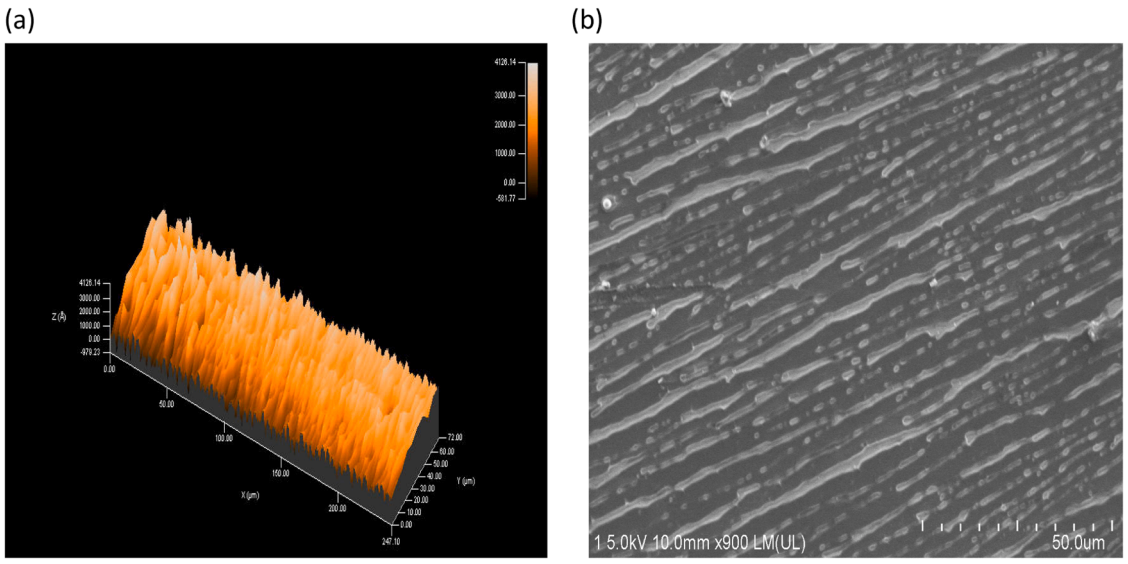

Fig. 3. (a) 3D pattern created on the glass substrate by self-alignment of short DNA oligomer and SWCNT(b) SEM image of parallel self-alignment of Poly(dT)20 and SWCNT created on the glass substrate.

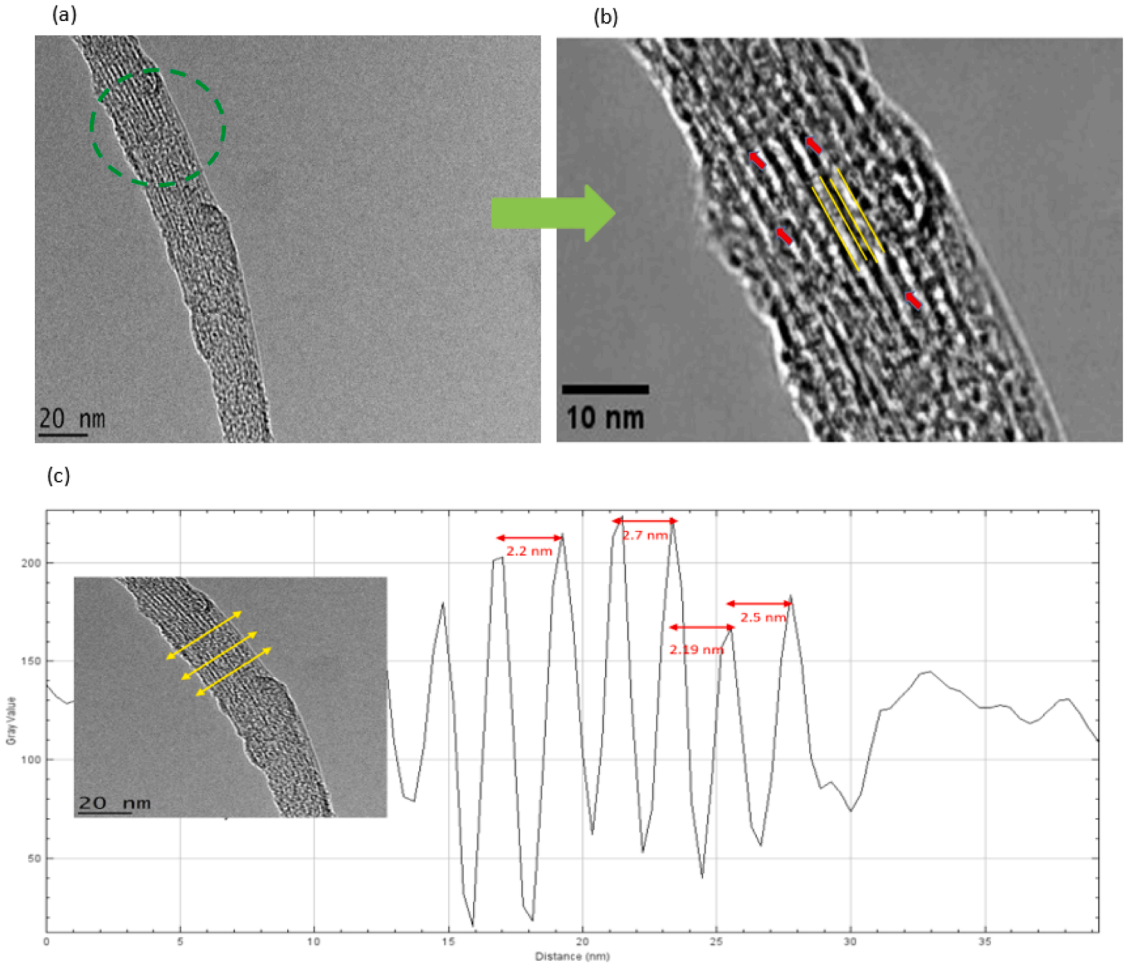

Fig. 4. (a) HRTEM image of short length poly(dT)20 (b) poly(dT)20 (red arrow indicate) around SWCNT (yellow parallel line) and (c) Lateral profile along yellow arrow direction.

the nanotubes and amplifying repulsive interactions [41]. Lateral line profiles were extracted from the magnified HRTEM image (sub-Fig. 4(c)) along the yellow arrow direction using ImageJ software. These profiles were analyzed to assess the alignment of the SWCNTs and measure their diameters. As illustrated in Fig. 4(c), the lateral profile of the Poly(dT) 20/SWCNT exhibits a closely uniform wave shape, indicating that it is

well-aligned. The diameters, measured along the yellow arrow after scale calibration using ImageJ software, are approximately 2.2 nm, 2.7 nm, 2.19 nm, and 2.5 nm. The process for drawing the lateral profile curve and measuring the diameter using ImageJ software involves several key steps: First, open the image and set the scale by drawing a line over a known distance (using the scale bar in the image) and calibrating it through Analyze > Set Scale. Next, use the line tool to draw a line perpendicular to the SWCNT alignment, then generate the lateral profile by selecting Analyze > Plot Profile (or Ctrl + K) to obtain a graph of intensity values. To measure the diameter, identify the peaks and troughs in the plot profile by drawing a line from peak to peak, and use the Ctrl + M key combination to measure the length, which will then appear in the results table.

3.3. FTIR spectroscopy

Fourier Transform Infrared (FTIR) spectroscopy is widely used in various fields, including biology,materials science, and chemistry that can Provides information about vibrational modes of molecules, changes in bond strengths and molecular interactions. FTIR spectroscopy was utilized to describe the interaction between dpoly(T)20 and SWCNTs in order to assess SWCNT vibration (Fig. 5). The presence of a C = O vibration at 1720 cm^{-1} and 2890 cm^{-1} in the FTIR spectra (dashed circle in Fig. 5) suggests an interaction between the poly(dT)20 and SWCNTs. This vibrational mode, characteristic of carbonyl groups, indicates that the poly(dT)20 molecules are likely attached to the SWCNTs through the formation of bonds between the C = O groups and the carbon atoms on the SWCNT surface [42].

3.4. UV–Vis spectroscopy

UV–Vis spectroscopy is a powerful technique that can provide valuable insights into the structure, properties, and interactions of molecules. Fig. 6 depicts the UV–Vis absorption spectra of dpoly(T)20 and SWCNT, as well as their dpoly(T)20/SWCNT supermolecule, after ice bath sonication (t0 and t1) and two days of incubation (t2 and t3). The observed spectral shifts confirm the binding between dpoly(T)20 and SWCNT, primarily attributed to π-π stacking, electrostatic interactions and hydrophobic Force. The strong local electric field generated along the SWCNT axis can further influence the DNA's electronic structure, potentially causing shifts or the appearance of new peaks in the absorption spectrum [10,20].

The observed spectral changes in dpoly$(dT)_{20}$, specifically the reduction in the 270 nm peak and the emergence of a new peak at 390–400 nm (indicated by a dash-dot line circle in the Fig. 6), provide strong evidence for an interaction with SWCNT that can create a more stable structure forming between dpoly$(dT)_{20}$ and SWCNT.

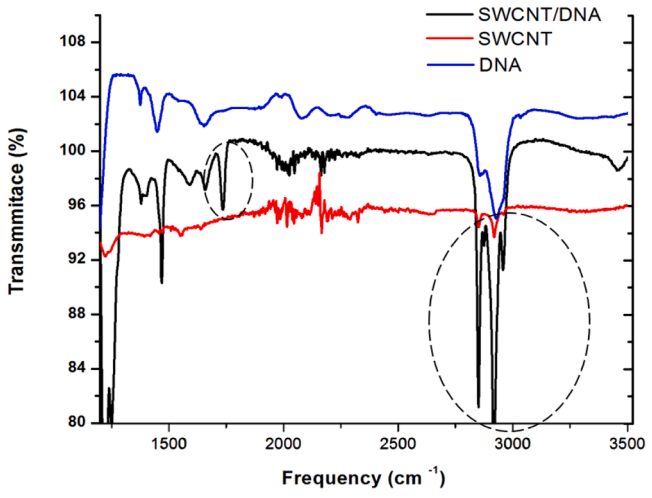

Fig. 5. Typical Fourier-transform infrared spectra of SWCNT (red line), dpoly (T)20 (blue line) and dpoly(T)20 /SWCNT (black line); The dashed circle at 1720 cm^{-1} & 2890 cm^{-1} show the C = O vibration.

3.5. Polarization of poly(dT)20 /SWCNT

A rotational stage is employed to evaluate the alignment of poly(dT) 20/SWCNT complexes in Raman spectroscopy, utilizing a polarized confocal Raman microscope equipped with a 514 nm laser (Fig. 7(a)). The Raman spectrometer was calibrated, and the rotation stage was mounted on a stable platform to minimize vibrations. The poly(dT)20 /SWCNT array on galss substrate carefully placed on the rotation stage. Initially, the stage was set to a zero-degree angle, serving as the reference point for alignment (Using a microscope attached to the Raman system, the poly(dT)20 /SWCNT orientation determined). The poly(dT) 20 /SWCNT) on 1 cm x 1 cm substrate were aligned parallel to the global axis of the rotation stage (Fig. 7(a)). Subsequently, the stage gradually rotated from the zero-degree angle while monitoring the Raman signal intensity, specifically focusing on G bands associated with the SWCNTs. Fig. 7(b) provides a high-resolution transmission electron microscopy (HRTEM) image of these AuNPs. Gold nanoparticles (AuNPs) of 3–5 nm (Red arrow in the Fig. 7(b)) were employed to enhance Raman spectra.

The single-walled carbon nanotubes (SWCNTs) are deposited on a glass substrate that is fixed onto a rotational stage, ensuring that the is aligned consistently with the orientation of the SWCNTs during rotation. This setup allows for precise control over the alignment and orientation of the SWCNTs, facilitating experiments that require specific directional properties or interactions. The angle formed between the polarization direction of the incoming light (e2) and the alignment direction of the SWCNT (e1) is represented by α.

As predicted in the Fig. 8(a), when e_1 is parallel to e_2 ($e_1 \parallel e_2$), the intensity of Raman scattering is maximum and on the other hand when the relative angle is 90o ($e_1 \perp e_2$), the intensity of Raman scattering is at its minimum value. To further investigate the angle-dependent arrangement of poly(dT)20/SWCNT complexes, Raman spectra were acquired over a frequency range of 150–1600 cm^{-1}, focusing on the G-band region. These measurements were conducted at 15 different angles, ranging from 0 to 360° (Fig. 8(a)). The polar diagram illustrates the G band intensity of poly(dT)20 /SWCNT arrays as a function of the angle

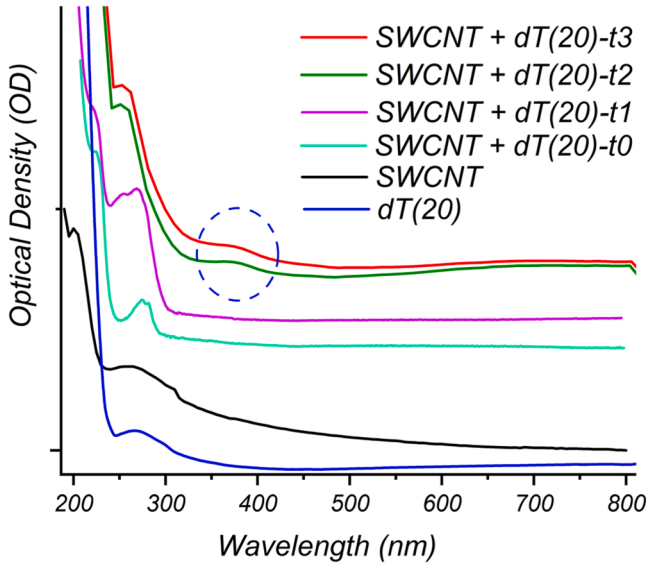

Fig. 6. UV–Vis spectra of dpoly(T)20 and SWCNT, after ice bath sonication (t0 and t1) and after two days of incubation (t2 and t3) (Combining multiple graphs into a single diagram, with move only y-axis,for better visualiziong the peaks comparison).

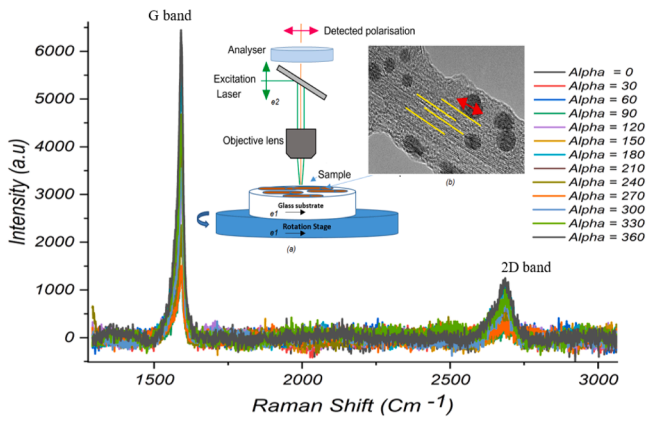

Fig. 7. The Raman spectra of DNA-wrapped single-walled carbon nanotube for different angles of light polarization. Subfigure (a) The experimental setup of polarized Raman spectroscopy (b) HRTEM image wrapping short length DNA (red arrow indicate) and SWCNTs alingment (yellow parallel line).

between e_1 and e_2 (Fig. 8(b)). The polar diagram reveals that the intensity of the G band is strongly influenced by the orientation of the SWCNTs, and this relationship is directly proportional to the square of the cosine of the angle between the polarization direction of the incident light (e_1) and the SWCNT alignment direction (e_2) (α) [43,44].

The angular dependences of the Raman intensities (I) was futher evaluated by cosine operator relation of the angle between e_1 and e_2 base on the equation ($I(\alpha) = I_0 * \cos^2(\alpha)$) [44] where I(α) is the intensity of the G peak in the Rraman spectrum at angle α, I_0 is the maximum intensity and α is the angle between the poly(dT)$_{20}$ /SWCNT axis and polarization direction. Fig. 9 illustrates the G band intensity of Raman spectra via (Cos ^{2}α) which clearly shows a linear relationship between I and Cos ^{2} α (R-squared value of 0.9, indicating a strong). This linear relationship, in which the angle between the incident light and the material alignment determines the intensity of the Raman signal, is also suggestive of a well-aligned material.

The intensity ratio between the perpendicular and parallel poly(dT) 20/SWCNT arrays, measured using polarized Raman spectroscopy, yields the depolarization ratio, $r = \frac{I_{Perpmdecular}}{I_{Parallel}}$. This ratio is dependent on the molecular symmetry of the material [45–47]. The average depolarization ratio of 0.211 indicates a well-oriented poly(dT)20/SWCNT structure. A lower depolarization ratio signifies a higher degree of alignment within the material [48].

4. Conclusions and future direction

n this study, the innovative application of light polarization in conjunction with DNA homopolymer-coated, single-wall carbon nanotubes (SWCNTs) has been successfully demonstrated through a sophisticated optical setup that incorporates polarized laser light and a rotational stage. Utilizing chemical preparation of SWCNT surface and sonication, the poly(dT)20, was effectively wrapped around the SWCNTs, resulting in the formation of a uniform pattern. Experimental findings, corroborated by Fourier-transform infrared (FTIR) and ultraviolet-visible (UV–Vis) spectroscopy, confirm the presence of interactions between the SWCNTs and the poly(dT)20, facilitating the emergence of parallel structures. Comprehensive morphological and structural analyses conducted using high-resolution techniques, such as high-resolution transmission electron microscopy (HRTEM) and field emission scanning electron microscopy (FESEM), provide compelling evidence of the parallel geometry of the SWCNTs. Additionally, polarized Raman spectroscopy with a 514 nm laser was employed to investigate the variation of the G-band as a function of the rotational angle, substantiating the parallel alignment of the poly(dT)20/SWCNT structure. The observed depolarization ratio of approximately 0.211 and linear relationship between I and Cos ^{2} (α) serves as a robust indicator of

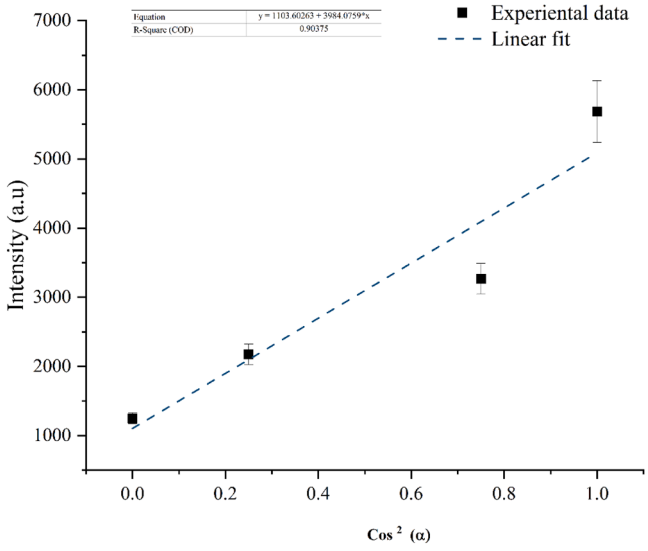

Fig. 9. Raman scattered light intensity vs. cos^2(α) for DNA-wrapped single-walled carbon nanotube.

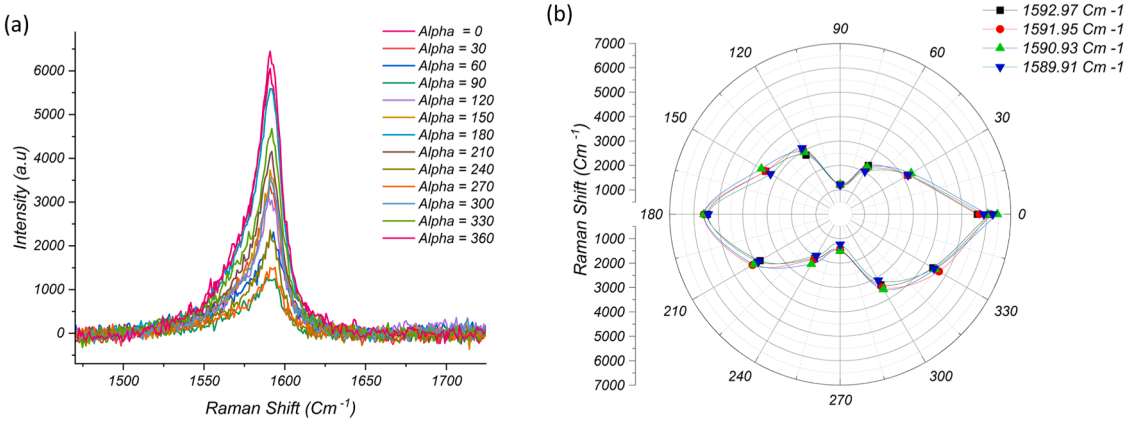

Fig. 8. (a) Polarized Raman spectra of the G band of poly(dT)20 /SWCNT as a function of the polarization angle α (b) A polar plot of the poly(dT)20 /SWCNT array G band Raman intensity at 1591.95 cm^{-1}, 1592.97 cm^{-1}, 1590.93 cm^{-1} and 1589.9 1cm^{-1} (The line represents the trend line, while the markers indicate the experimental data points).

the high degree of alignment achieved in this study. The HRTEM image verifies that the binding of 20-mer thymine to single-walled carbon nanotubes (SWCNTs) through a wrapping mechanism creates steric hindrance, effectively distancing the nanotubes and inhibiting aggregation. The aligned structure of the poly(dT)20/SWCNT structure presents significant potential for a wide array of applications, particularly in the advancement of detection platforms for biosensors and optical sensing devices. The anisotropic properties inherent in these complexes can be strategically harnessed to enhance the sensitivity and specificity of biosensing technologies in future endeavors.

CRediT authorship contribution statement

Seyedeh Maryam Banihashemian: Writing – original draft, Validation, Methodology, Investigation, Formal analysis, Data curation. **Mohsen Mesbah:** Writing – review & editing, Visualization, Validation, Software, Conceptualization. **Hesam Kamyab:** Writing – review & editing, Visualization, Validation, Supervision, Formal analysis, Conceptualization. **Mohammad Mahdi Taheri:** Writing – review & editing, Visualization, Software, Investigation, Formal analysis, Conceptualization. **Balamuralikrishnan Balasubramanian:** Writing – review & editing, Visualization, Validation, Software, Investigation, Conceptualization.

Declaration of competing interest

The authors declare that they have no known competing financial interests or personal relationships that could have appeared to influence the work reported in this paper.

Acknowledgements

This research was supported by the Iran National Science Foundation (INSF) grant number (94026093).

Data availability

Data will be made available on request.

References

[1] M.M. Bhanjadeo, A.K. Nayak, U. Subudhi, Surface-assisted DNA self-assembly: an enzyme-free strategy towards formation of branched DNA lattice, Biochem. Biophys. Res. Commun. 485 (2) (2017) 492–498.
[2] N. Tokumitsu, Y. Shimamura, T. Fujii, Y. Inoue, Effect of Annealing and Diameter on Tensile Property of Spinnable Carbon Nanotube and Unidirectional Carbon Nanotube Reinforced Epoxy Composite, J. Compos. Sci. 6 (12) (2022) 389.
[3] B. Nayak, R. Mondal, and M.O.J.N. Thotiyl, "Electrostatically driven unidirectional molecular flux for high performance alkaline flow batteries," vol. 15, no. 35, pp. 14468–14475, 2023.
[4] T. Arumugham", et al., Preparation and characterisation of porous activated carbon using potassium hydroxide chemical activation with ultrasonic association, Biomass Convers. Biorefin. (2023) 1–13.
[5] S. Abdulla and B.J.L. Pullithadathil, "Unidirectional Langmuir–Blodgett-mediated alignment of polyaniline-functionalized multiwalled carbon nanotubes for NH3 gas sensor applications," vol. 36, no. 39, pp. 11618–11628, 2020.
[6] A. Amani, et al., Multifunctional MXenes nanocomposite platforms for biosensing and wearable sensor technologies, Adv. Compos. Hybrid Mater. 8 (2025) 1–26.
[7] S.M. Banihashemian, H. Hajghassem, A. Nikfarjam, J. Azizi Jormoshti, S. Abdul Rahman, G. Boon Tong, Room temperature ethanol sensing by Green Synthesized Silver nanoparticle decorated SWCNT, Sens. Actuat. B: Chem. (2018) not published.
[8] X. Lu et al., "Fabrication of bio-inspired anisotropic structures from biopolymers for biomedical applications: a review," vol. 308, p. 120669, 2023.
[9] J.P. Jahnke et al., "Mesostructured Materials with Controllable Long-Range Orientational Ordering and Anisotropic Properties," vol. 35, no. 51, p. 2306800, 2023.
[10] G. Sánchez-Pomales, C. Pagán-Miranda, L. Santiago-Rodríguez, C.R. Cabrera, DNA-wrapped carbon nanotubes: from synthesis to applications. Carbon Nanotubes, InTech, 2010.
[11] S.R. Lustig, A. Jagota, C. Khripin, M. Zheng, Theory of structure-based carbon nanotube separations by ion-exchange chromatography of DNA/CNT hybrids, J. Phys. Chem. B 109 (7) (2005) 2559–2566, 2005/02.
[12] H. Gao, Y. Kong, Simulation of DNA-nanotube interactions, Annu. Rev. Mater. Res. 34 (2004) 123–150.
[13] H.T. Maune, et al., Self-assembly of carbon nanotubes into two-dimensional geometries using DNA origami templates, Nat. Nano 5 (1) (2010) 61–66.
[14] P. He, L. Dai, Aligned carbon nanotube–DNA electrochemical sensors, Chem. Commun. 3 (3) (2004) 348–349.
[15] R. Singh, et al., Binding and condensation of plasmid DNA onto functionalized carbon nanotubes: toward the construction of nanotube-based gene delivery vectors, J. Am. Chem. Soc. 127 (12) (2005) 4388–4396.
[16] W. Zhao, Y. Gao, M.A. Brook, Y. Li, Wrapping single-walled carbon nanotubes with long single-stranded DNA molecules produced by rolling circle amplification, Chem. Commun. (34) (2006) 3582–3584.
[17] X. Zhao, J.K. Johnson, Simulation of adsorption of DNA on carbon nanotubes, J. Am. Chem. Soc. 129 (34) (2007) 10438–10445.
[18] C. Khripin, M. Zheng, A. Jagota, Deposition and meniscus alignment of DNA–CNT on a substrate, J. Colloid Interface Sci. 330 (2) (2009) 255–265.
[19] B. Wei, et al., Regulation of DNA self-assembly and DNA hybridization by chiral molecules with corresponding biosensor applications, Anal. Chem. 87 (4) (2015) 2058–2062, 2015/02/04.
[20] S. Meng, E. Kaxiras, Interaction of DNA with CNTs: properties and prospects for electronic sequencing, Biosens. Using Nanomater. (2009) 67r96.
[21] M.E. Hughes, E. Brandin, J.A. Golovchenko, Optical absorption of DNA-carbon nanotube structures, Nano Lett. 7 (5) (2007) 1191–1194.
[22] O. Cavuslar, H. Unal, Self-assembly of DNA wrapped carbon nanotubes and asymmetrical cyanine dyes into fluorescent nanohybrids, RSC Adv. 5 (29) (2015) 22380–22389.
[23] Z. Liu, C. Tian, J. Yu, Y. Li, W. Jiang, C. Mao, Self-assembly of responsive multilayered DNA nanocages, J. Am. Chem. Soc. 137 (5) (2015) 1730–1733, 2015/01/28.
[24] S. Jessl, S. Engelke, D. Copic, J.J. Baumberg, M. De Volder, Anisotropic carbon nanotube structures with high aspect ratio nanopores for Li-ion battery anodes, ACS Appl. Nano Mater. 4 (6) (2021) 6299–6305.
[25] P. Liu et al., "High-performance electric and optical biosensors based on single-walled carbon nanotubes," vol. 250, p. 119084, 2022.
[26] A. Ali, S.S.R. Koloor, A.H. Alshehri, A. Arockiarajan, Carbon nanotube characteristics and enhancement effects on the mechanical features of polymer-based materials and structures–A review, J. J. o. M. R. , and Technol. 24 (2023) 6495–6521.
[27] E. Leppänen, E. Gustafsson, N. Wester, I. Varjos, S. Sainio, and T.J.E.A. Laurila, "Geometrical and chemical effects on the electrochemistry of single-wall carbon nanotube (SWCNT) network electrodes," vol. 466, p. 143059, 2023.
[28] G. SAnchez-Pomales, L. Santiago-RodrAguez, and C.R. Cabrera, "DND-Assisted Purification and Self-Assembly of Single-Walled Carbon Nanotubes on Gold," 2006.
[29] B. Xu, N. Mao, Y. Zhao, L. Tong, J. Zhang, Polarized Raman spectroscopy for determining crystallographic orientation of low-dimensional materials, J. Phys. Chem. Lett. 12 (31) (2021) 7442–7452, 2021/08/12.
[30] Y. Li, W. Shi, and N.J.C. Chopra, "Functionalization of multilayer carbon shell-encapsulated gold nanoparticles for surface-enhanced Raman scattering sensing and DNA immobilization," vol. 100, pp. 165–177, 2016.
[31] A.Y. Glamazda, A. Plokhotnichenko, V. Leontiev, V. Karachevtsev, DNA-wrapped carbon nanotubes aligned in stretched gelatin films: polarized resonance Raman and absorption spectroscopy study, Phys. E: Low-Dimens. Syst. Nanostruct. 93 (2017) 92–96.
[32] J. Wu, N. Mao, L. Xie, H. Xu, and J.J.A.C. Zhang, "Identifying the crystalline orientation of black phosphorus using angle-resolved polarized Raman spectroscopy," vol. 54 8, pp. 2366–9, 2015.
[33] L. Liu et al., "Aligned, high-density semiconducting carbon nanotube arrays for high-performance electronics," vol. 368, pp. 850–856, 2020.
[34] S. Yu, X. Li, W. Lu, H. Li, Y.V. Fu, F. Liu, Analysis of Raman spectra by using deep learning methods in the identification of marine pathogens, Anal. Chem. 93 (32) (2021) 11089–11098, 2021/8/17.
[35] O. Ambartsumyan, D. Gribanyov, V. Kukushkin, A. Kopylov, E. Zavyalova, SERS-based biosensors for virus determination with oligonucleotides as recognition elements, Int. J. Mol. Sci. 21 (9) (2020) 3373, 2020/5/10.
[36] V. Nagyte, et al., Raman fingerprints of graphene produced by anodic electrochemical exfoliation, Nano Lett. 20 (5) (2020) 3411–3419, 2020/5/13.
[37] A. Roberts, et al., A recent update on advanced molecular diagnostic techniques for COVID-19 pandemic: an overview, Front. Immunol. 12 (2021) 732756, 2021/12/14.
[38] Y. Saito, T. Kondo, S. Harada, R. Kitaura, M.V. Balois-Oguchi, N. Hayazawa, Intermolecular Interaction between Single-Walled Carbon Nanotubes and Encapsulated Molecules Studied by Polarization Resonance Raman Microscopy, J. T. j. o. p. c. B. (2023).
[39] Y. Zhang, Z. Song, L. Miao, Y. Lv, L. Gan, M. Liu, All-round enhancement in Zn-ion storage enabled by solvent-guided Lewis acid-base self-assembly of heterodiatomic carbon nanotubes, ACS Appl. Mater. Interface. 15 (29) (2023) 35380–35390, 2023/7/26.
[40] L. Golubewa, I. Timoshchenko, and T.J.T.A. Kulahava, "Specificity of carbon nanotube accumulation and distribution in cancer cells revealed by K-means clustering and principal component analysis of Raman spectra," 2024.
[41] J. Wang and T. Lei, "Separation of Semiconducting Carbon Nanotubes Using Conjugated Polymer Wrapping," vol. 12, no. 7, p. 1548, 2020.
[42] K. Awasthi, D. Singh, S.K. Singh, D. Dash, O. Srivastava, Attachment of biomolecules (protein and DNA) to amino-functionalized carbon nanotubes, New Carbon Mater. 24 (4) (2009) 301–306.

[43] M. Wang et al., "Raman antenna effect from exciton-phonon coupling in organic semiconducting nanobelts," vol. 9 48, pp. 19328–19336, 2017.
[44] F. Roussel, J.-F. Brun, A. Allart, L. Huang, S. O'Brien, Horizontally-aligned carbon nanotubes arrays and their interactions with liquid crystal molecules: physical characteristics and display applications, AIP Adv. 2 (1) (2012).
[45] G.S. Duesberg, I. Loa, M. Burghard, K. Syassen, S. Roth, Polarized Raman Spectroscopy on Isolated Single-Wall Carbon Nanotubes, Phys. Rev. Lett. 85 (25) (2000) 5436–5439, 2000/12/18.
[46] X.-L. Liu, X. Zhang, M.L. Lin, P. Tan, Different angle-resolved polarization configurations of Raman spectroscopy: a case on the basal and edge plane of two-dimensional materials*, J. C. P. B. 26 (2017) 067802.
[47] U.B. Ramabadran, B.J.M.S. Roughani, Intensity analysis of polarized Raman spectra for off axis single crystal silicon, E. B.-a. F. S.-s. Materials 230 (2018) 31–42.
[48] S. Hao, H. Li, X. Li, L. Li, J. Xie, Effect of impurity content on structure of living water, J. J. o. W. C. and Technol. 38 (2016) 158–162.